REVIEWS

Journal of Semiconductors
(2020) 41, 091701
doi: 10.1088/1674-4926/41/9/091701

Optoelectronic and photocatalytic properties of I–III–VI QDs: Bridging between traditional and emerging new QDs

Yanhong Liu[1, ‡], Fenghua Li[1, ‡], Hui Huang[2], Baodong Mao[1, †], Yang Liu[2, †], and Zhenhui Kang[2, †]

[1]Institute of Green Chemistry & Chemical Technology, School of Chemistry and Chemical Engineering, Jiangsu University, Zhenjiang 212013, China

[2]Institute of Functional Nano and Soft Materials (FUNSOM), Jiangsu Key Laboratory for Carbon-based Functional Materials and Devices, Soochow University, Suzhou 215123, China

Abstract: Due to the quantum size effect and other unique photoelectric properties, quantum dots (QDs) have attracted tremendous interest in nanoscience, leading a lot of milestone works. Meantime, the scope and scientific connotation of QDs are constantly expanding, which demonstrated amazing development vitality. Besides the well-developed Cd-containing II–VI semiconductors, QDs of environmentally friendly I–III–VI (I = Cu, Ag; III = Ga, In; VI = S, Se) chalcogenides have been a hot spot in the QDs family, which are different from traditional II–VI QDs in terms of multi-composition, complex defect structure, synthetic chemistry and optical properties, bringing a series of new laws, new phenomena and new challenges. The composition of I–III–VI chalcogenides and their solid solutions can be adjusted within a very large range while the anion framework remains stable, giving them excellent capability of photoelectric property manipulation. The important features of I–III–VI QDs include wide-range bandgap tuning, large Stokes shift and long photoluminescence (PL) lifetime, which are crucial for biological, optoelectronic and energy applications. This is due to the coexistence of two or more metal cations leading to a large number of intrinsic defects within the crystal lattice also known as deep-donor-acceptor states, besides the commonly observed surface defects in all QDs. However, a profound understanding of their structure and optoelectronic properties remains a huge challenge with many key issues unclear. On one hand, the achievements and experience of traditional QD research are expected to provide vital value for further development of I–III–VI QDs. On the other hand, the understanding of the emerging new QDs, such as carbon and other 2D materials, are even more challenging because of the dramatically different composition and structure from II–VI semiconductors. For this, I–III–VI QDs, as a close relative to II–VI QDs but with much more complex composition and structure variation, provide a great opportunity as a gradual bridge to make up the big gap between traditional QDs and emerging new QDs, such as carbon dots. Here, we hope to compare the research progress of I–III–VI QDs and II–VI QDs, in an effort to comprehensively understand their structure, synthetic chemistry, optical electronic and photocatalytic properties. We further give insights on the key potential issues of I–III–VI QDs from the perspective of bridging between traditional QDs and emerging carbon dots, especially the profound principles behind synthetic chemistry, PL mechanism and optoelectronic applications.

Key words: I–III–VI; II–VI; quantum dots; carbon dots; optical properties; photocatalysis

Citation: Y H Liu, F H Li, H Huang, B D Mao, Y Liu, and Z H Kang, Optoelectronic and photocatalytic properties of I–III–VI QDs: Bridging between traditional and emerging new QDs[J]. *J. Semicond.*, 2020, 41(9), 091701. http://doi.org/10.1088/1674-4926/41/9/091701

1. Introduction

Colloidal quantum dots (QDs) refer to the uniform small semiconductor particles, in which the charge carrier transportation is confined by three dimensions[1]. As a result, of the small size, the continuous energy band becomes discrete energy levels together with series of unique photoelectric properties, known as the quantum confinement effect. QDs have played a central role in the development of nanoscience with several related milestone works, such as the discovery of quantum size effect[2–4], size controllable synthesis[5, 6], biology[7–9] and device applications[10, 11]. Nearly 40 years later, it continues research to be a hot topic in nanoscience, while the connotation of the QDs family is constantly expanding, showing amazing development vitality. Traditionally, QDs field mainly focused on II–VI and IV–VI semiconductors containing heavy metals. Now, environmentally friendly I–III–VI (I = Cu, Ag; III = Ga, In; VI = S, Se) QDs have attracted more and more attention as an important subset of the QD family[12, 13]. In a certain sense, I–III–VI QDs can be considered as a substitute structure by replacing the +2 cations (such as Cd) in II–VI chalcogenides with +1 and +3 cations. However, they are different in several aspects from traditional II–VI QDs due to the complex nature of nonstoichiometric composition and crystal structure, which brings a series of new laws, new phenomena and new challenges to the fulfillment of the whole QDs field, especially on synthetic chemistry and photoluminescence (PL) properties. More importantly, QDs play an irreplaceable role as the structural and catalytic model systems in understanding and demonstrating the unique laws on the nano-

Yanhong Liu and Fenghua Li contributed equally to this work.
Correspondence to: B D Mao, maobd@ujs.edu.cn; Y Liu, yangl@suda.edu.cn; Z H Kang, zhkang@suda.edu.cn
Received 1 AUGUST 2020; Revised 20 AUGUST 2020.

scale between lay atomic and bulk materials. As Prof. Feynman pointed out half a century ago, 'there is plenty of room at the bottom', which was first demonstrated with II–VI semiconductor system. Now, when it is expanded to more and more emerging new materials, such as carbon and other 2D materials, the large gap on composition and structure imposes series of great challenges on the synthetic manipulation, optical properties and mechanism understanding. From this aspect, I–III–VI QDs, as a close relative to II–VI QDs but with much more complex composition and structure variation, provides a great opportunity as a gradual bridge to make up the big gap between traditional QDs and emerging new QDs, such as carbon dots.

I–III–VI chalcogenides and their solid solutions have the advantages of low toxicity and continuously adjustable band gap covering the UV–vis to near infrared region which has attracted huge amount of attention as promising alternatives to the traditional cadmium- or lead-containing QDs[14, 15]. These I–III–VI chalcogenides are usually direct bandgap semiconductors with strong light absorption[16, 17]. Early research of I–III–VI compounds were focusing on thin films[18, 19] and nanoparticles[20] for solar cell applications[21]. Recently, the excellent optical properties have made these non-toxic I–III–VI QDs useful in bioimaging, light-emitting diodes (LEDs), and photocatalysis etc. The composition of these multinary chalcogenides can be adjusted in a very large range while the anion skeleton remains stable, which brings excellent control ability of the optical and electrical properties[22]. The important features include widely adjustable bandgap and long PL lifetime that are the key to related applications in devices and biological systems. However, this also brings the difficulties on the synthesis of uniform particles with well-controlled composition and size. Moreover, the coexistence of two or more cations bring abundant inner defects, together with the surface defects, resulting in high-density trap states and significantly different optoelectronic properties from II–VI QDs and imposing new challenges on related applications.

QDs have played a key role in many fields such as biology, devices and catalysis. Among these application, photocatalysis, as potentially the key solution to both environmental and energy problems, has been the most prominent and widely studied field not only for traditional QDs, but also for I–III–VI QDs and carbon dots[23]. As a class of widely used semiconductor materials, I–III–VI QDs are more like a close relative of the traditional II–VI QDs and are naturally similar in terms of roots and research methods[24]. In the development process, it also obtained a lot of experience from II–VI QDs. For the recently emerged QDs, such as carbon dots, there is a great gap in structure and properties and subsequently more research challenges from that of II–VI QDs. Considering this, I–III–VI QDs provide an important gradient bridge for these emerging new QDs, to better understand their new photoelectric properties, challenges and development process. As we summarized earlier, it lacks transition and bridge from the traditional inorganic II–VI semiconductors to the complicated pseudo-organic/biological carbon dots system, which imposes great challenges on comparison and correlation of their structure, optoelectrical properties and applications. Relatively speaking, there are many reviews of traditional QDs and emerging carbon dots, but fewer reviews of I–III–VI QDs.

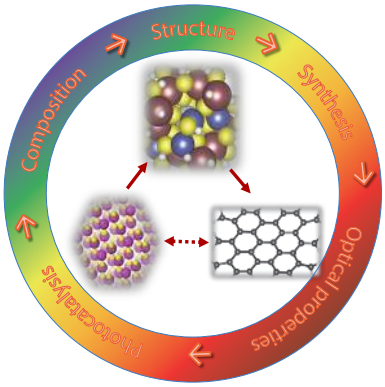

Fig. 1. (Color online) Schematic illustration for the bridging role of I–III–VI QDs between traditional II–VI QDs and emerging new carbon dots.

More importantly, there is no review article has summarized this field in the perspective of bridging between traditional QDs and emerging new carbon dots. So, here we try to give a brief review of I–III–VI QDs focusing on the discussion of their photoelectric and photocatalytic properties in systematic comparison with traditional QDs, and also give a short perspective of their key bridging role in the whole QDs family (Fig. 1). More efforts were contributed to resulted from challenges and issues the multinary composition in I–III–VI QDs, such as the complicated structural characteristics, balancing reactivity during synthetic process, optical properties dominated by abundant defect states, the crucial role of the long-lived charge carriers, and engineering of the bandgap and trap states in photocatalysis.

2. Structure

I–III–VI chalcogenides constitute a large class of semiconductor materials, whose band gap can be tuned not only by size and shape, but also by continuous composition manipulation[15, 25]. The classic composition of bulk I–III–VI semiconductors is I–III–VI_2, but there are also some I–III_5–VI_8 compounds. Most importantly, their composition can be continuously adjusted in a large range without affecting the stability of the anion framework[14]. Conceptually, the ternary I–III–VI chalcogenides can be made from II–VI materials by replacing two divalent Cd^{2+} with one monovalent (such as Cu^{+}) and one trivalent (such as In^{3+}) cation[26]. Crystal structure of the ternary I–III–VI QDs includes chalcopyrite, zinc blend, and hexagonal wurtzite phases[26]. However, the zinc blend and wurtzite phases usually can only be observed at high temperatures. In the chalcopyrite structure, the $M^{+}{}_2M^{3+}{}_2$ tetrahedron usually centered on the chalcogenide atoms[27]. Due to the coexistence of multi cations with different radius and deviation from the stoichiometry, I–III–VI QDs tend to form lots of internal defects, which act as deep donor-acceptor-pair (DAP) trap states for charge carriers and thus form the characteristic PL from DAP recombination[28]. This is the biggest difference between I–III–VI and traditional II–VI QDs that mainly containing surface defects. As an example, the defect sites in chalcopyrite $CuInS_2$ QDs include sulfur vacancies (V_S), copper vacancies (V_{Cu}) and indium on copper sites (In_{Cu}), where the Cu-related defects are more easy to produce due to the relatively weaker Cu–S bonds than In–S[29].

The energy band structure of the multinary I–III–VI chalco-

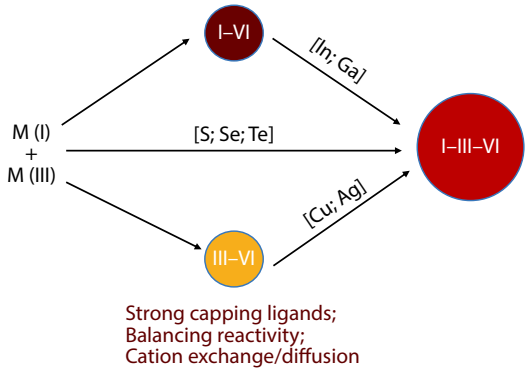

Fig. 2. (Color online) Schematic synthetic processes of I–III–VI QDs. Reprinted from Ref. [14].

genide compounds can be adjusted by the alloy composition, thereby affecting the light absorption and reducing capability[28]. Through theoretical calculation and analysis of energy band structure, it was found that Cu 3d and Ag 4d orbits, as part of the valence band (VB) composition, play a key role in increasing the VB level[30, 31]. The introduction of Zn 4s4p orbital improves the conduction band (CB) level and improves the reducing capability[32]. A large number of studies on I–III–VI QDs have shown adjusted band gap along with CB/VB positions to optimize the photocatalytic activity[14]. It is worth noting that in the current research, the quaternary alloy QDs of traditional cadmium chalcogenides have not been well developed. In contrast, QDs of I–III–VI-derived quaternary alloys have attracted great interest due to their promising properties as non-toxic substitutes for cadmium chalcogenides in various applications. Two kinds of quaternary alloys are derived from I–III–VI QDs, including the self-alloy within I–III–VI semiconductors (such as $CuIn_xGa_{1-x}Se_2S_8$ and $CuIn_xGa_{1-x}(S_{1-y}Se_y)$)[33, 34] and the alloy of I–III–VI semiconductor with zinc or cadmium chalcogenides (such as Cu–In–Zn–S[35] and Ag–In–Zn–S[36]), whose composition can all be manipulated flexibly.

3. Synthesis

The preparation method and growth mechanism of ternary and multinary I–III–VI QDs are similar to traditional binary II–VI QDs, since the basic synthetic principles are similar. Currently, the hot injection method is still the main synthesis strategy of the complex I–III–VI QDs containing three or more elements. The metal precursors and chalcogen precursors can be formed in the same way capped with corresponding ligands. The main synthesis challenge of I–III–VI QDs is the reactivity balancing of multiple metal cations with strong capping ligands, which is a prerequisite for the formation of particles with uniform composition, phase and controllable structure (Fig. 2)[37]. An example of the hot injection method of Zn_xCu_y-$InS_{1.5+x+0.5y}$ QDs is the reaction of metal acetate and sulfur in octadecene with oleic acid and dodecanethiol as capping reagents[38]. Strong coordination ligands are usually used to control the relative reactivity of different metal cations to ensure the growth of pure phase alloyed QDs[39]. It has also been reported that capping reagents, such as dodecane thiol, play a key role in forming pure phase QDs ($CuInS_2$) instead of composite QDs (Cu_2S and In_2S_3)[34]. Insufficient capping of metal precursors may lead to the preparation of phase or composition separation, and uniform QDs cannot be obtained. Cation or anion exchange is also used for I–III–VI QDs (Fig. 2), such as the preparation of uniform $CuInS_2$ QDs or $Cu_2S/CuInS_2$ heterojunctions starting from Cu_2S QDs[40, 41]. The conversion of the Cu_2S–$CuInS_2$ composite to phase-pure $CuInS_2$ QDs was also observed at an elevated temperature of 250 °C[42]. As an important member of I–III–VI QDs, $AgInS_2$ is usually reported as an analogue of $CuInS_2$ in the early studies. In 2007, ZnS–$AgInS_2$ was the first reported solid solution QDs with PL systematically adjusted by the amount of ZnS, which started to attract lots of attention to alloyed or solid solution QDs[43]. Recently, much work has also focused on the synthesis of $AgInS_2$ and $AgInS_2$–ZnS alloy QDs. $AgInS_2$ is slightly different because of the relatively high reactivity of Ag^+ with S, which requires strong protection of the precursors as well as low temperatures to ensure the controllable particle nucleation and growth[44].

Aqueous synthesis methods are receiving more and more attention because of the promising biological and catalytic applications of I–III–VI QDs. With mercaptoacetic acid, mercaptopropionic acid and other thiol-containing amines/alcohols as ligands, different types of I–III–VI QDs can be synthesized[45–47]. In addition, the microwave- and ultrasonic-assisted methods can further optimize the aqueous phase synthesis method that decompose reactants under high-frequency electromagnetic radiation and high temperature[48]. However, the QDs synthesized by the aqueous method usually have lower PL efficiency, larger size distribution, and subsequently PL tailing[49]. In addition, the simple thiol ligands have poor stability and tend to fall off the QDs surface, resulting in QDs aggregation and PL decrease. Of course, with more and more reliable methods developed to improve the quality of aqueous QDs, the green synthesis method using water as the solvent is still a very promising route[50–52]. Scale-up preparation of the I–III–VI QDs up to 4 L was also reported using a low-cost electric cooker[53]. To further improve the application potential, size-selective separation may be a key to improving the quality of multinary QDs in aqueous phase[54].

Semiconductor heterojunctions are critical in the bandgap engineering and wave function engineering of QDs. In the binary II–VI QD system, surface passivation by growing a larger band gap semiconductor shell, are used to decrease surface defects and improve PL quantum yield (QY)[55]. In the I–III–VI core/shell QDs, the weight of the long-lived component increases with extended lifetime, while the fast decay component decreases[56]. By comparing CdS and ZnS as shell materials, it was found that CdS has a better passivation effect with a higher QY and an almost single exponential decay, while the ZnS passivation still shows double exponential decay[57]. Due to its low toxicity, ZnS is still a commonly used coating shell material for improving the optical properties of QDs. However, it worth to mention that cation exchange is also often reported in the preparation of $CuInS_2$/ZnS or $AgInS_2$/ZnS core/shell QDs with blue-shifted PL, which is caused by zinc alloying or doping[58]. During the preparation of core-shell structure, cation exchange or diffusion often compete with formation of the ZnS or CdS shell. The low contrast of high-resolution transmission electron microscopy (HRTEM) between $CuInS_2$ and ZnS makes it difficult to distinguish the atomic structure of the interface[59]. These challenges have brought a lot of difficulties to the synthesis of QDs with specific composition, structure and size, but further in-depth research has also

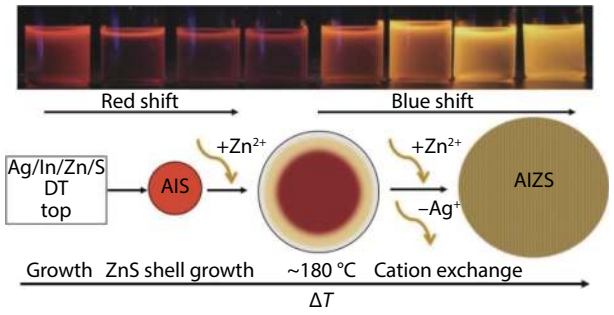

Fig. 3. (Color online) Schematic alloying and selective cation exchange process of quaternary $AgInS_2$–ZnS QDs. Reprinted from Ref. [60].

brought fruitful novel results on the regulation of photoelectric properties. For example, a series of $AgInS_2$–ZnS alloyed QDs were prepared with a programmed-temperature-increasing method (Fig. 3)[60]. The diffusion of wide-bandgap ZnS in $AgInS_2$–ZnS and the selective cation exchange of Zn for Ag were observed at increased temperatures. Spectroscopic studies show significantly improved PL QYs and ultra-long lifetime during alloying, and a new mechanism of structural evolution due to selective cation exchange was proposed. By systematically regulating the photoelectric properties of related doping and solid solution QDs, strategies such as selective cation exchange and controlled cation diffusion have resulted in the nearly ten times increase of the PL lifetime[60].

The declaration of particle growth mechanism played a crucial on the delicate control of QDs as well as the development of nanoscience and nanotechnology. In general, the related work of I–III–VI QDs preparation still cannot summarize out a clear nucleation and growth mechanism, especially the different aspects from that of II–VI QDs. It should be noted that although there have been a lot of reports on related research, the adjustment of the size distribution, surface structure and optical properties of I–III–VI QDs are still not comparable to that of II–VI QDs, and in-depth mechanism research is still lacking. This has brought a lot of challenges for the regulation of optoelectronic properties. Without compromising quality, mass production of ternary QDs remains a challenge, so optimized reactions that exceed laboratory scale is an urgent requirement. In order to achieve this goal, an in-depth understanding of chemical synthesis mechanism is necessary. From a basic scientific point of view, the precise structure and composition control is still challenging, which subsequently limits the manipulation and understanding of its optical properties. Comprehensive single-dot characterizations and spectroscopic measurements might be the key to clarify the correlation of optical performance and other physical parameters with structure. In addition, the synthesis and growth control research is carried out focusing on the ground state QDs, while the excited state mechanisms of these I–III–VI QDs are of great significance, especially their size, composition and surface/interface effects that are more critical in the design and preparation of photoelectric materials and clean energy applications (such as photovoltaics and photocatalysis).

4. Optical properties

4.1. Basic optical properties

There is no doubt that the I–III–VI QDs show the widest tunable optical properties due to changes in both size and composition. These materials also show special features, including longer excited state lifetimes, wider full width at half maximum (fwhm), larger Stokes shift, high quantum efficiency, along with simple and economical synthesis[39, 54, 56, 61–63]. Omata *et al.* calculated the size-dependent optical band gaps of I–III–VI chalcopyrite QDs with various compositions (Fig. 4(a)). The structure can be considered as metal cations embedded in the S/Se scaffold, similar to the structure of $Cu_{2-x}S$. The results agree well with the experimental values (Fig. 4(b)) and show that I–III–VI QDs can cover almost the entire spectral range from UV to near-infrared (NIR) by adjusting their composition and size. This shows the great potential of I–III–VI semiconductors as non-toxic QDs without heavy metals[25].

4.2. Mechanisms and defect states

The I–III–VI materials have photoelectric properties that are significantly different from traditional II–VI QDs, where the clarification of the excited state photophysical properties is crucial. The most important feature of I–III–VI QDs is their deep donor–acceptor pairs (DAPs, Fig. 5), which results in wide PL peaks and relatively large Stokes shifts. DAPs consist of different types of defects such as vacancies (V_{Cu} and V_S), interstitial atoms (Cu_i) and substituting (Cu_{In}), which are abundant in these ternary semiconductors due to the coexistence of multiple cations in the crystal lattice[64]. The deep donor–acceptor state has advantages such as long PL lifetimes, along with the low toxicity of these materials is crucial for related applications. Mao *et al.* used femtosecond transient absorption spectroscopy to identify the ultra-long lifetime of their excited states in ternary $AgInS_2$ QDs, which are of great significance for photoelectric conversion applications. They also systematically studied the PL lifetime of QDs of different sizes (1.9–3.1 nm) in the full spectral range, which clarified the source of its long-lived excited states and the different contribution of surface defects and internal defects (e.g. DAPs). They found that high-energy surface trap states are short-lived, and low-energy intrinsic trap states (e.g. DAPs) are long-lived. The ratio of surface trap states decreases with increasing particle size[65].

For chalcopyrite $CuInS_2$ QDs, the main contributions of optical transitions are assigned to the electrons at V_S and In_{Cu}, and holes at V_{Cu}[68]. Since the relatively weaker Cu–S bonds than In–S, Cu defects are more prone to the inversion defects[29]. The early PL studies show that the peak energy of different spectral components shifts to lower energy as the delay time increases[69, 70], a characteristic of DAP-related emission. In recent years, researches on the transient absorption spectroscopy, excitation power dependence, and time-resolved PL of $CuInS_2$ QDs have gradually developed toward the direction of "free-constraint" mechanism. The electrons are delocalized in CB, and the holes are located on Cu^+ or point defects that are generally considered to be V_{Cu}. For band gap engineering[71], thanks to the strong foundation of the traditional I–III–VI semiconductor industry, basic physical parameters such as CB, VB, bulk band gap, mobility, n-/p-doping and other information are relatively clear. However, due to the influence of the points and the size together, the mechanism research of QDs and the control of photoelectric properties are still far behind those of II–VI group QDs. For some

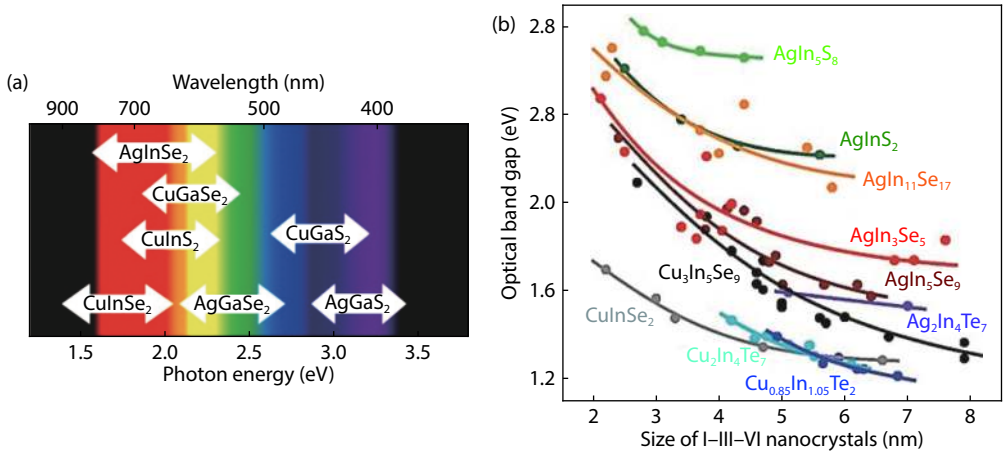

Fig. 4. (Color online) (a) Theoretical calculated[25] and (b) experimental results[14] of the size-dependent optical band gap of chalcopyrite I–III–VI semiconductor QDs. The band gaps in panel (a) were calculated based on QDs with sizes of 2 to 5 nm. Reprinted from Refs. [14, 25].

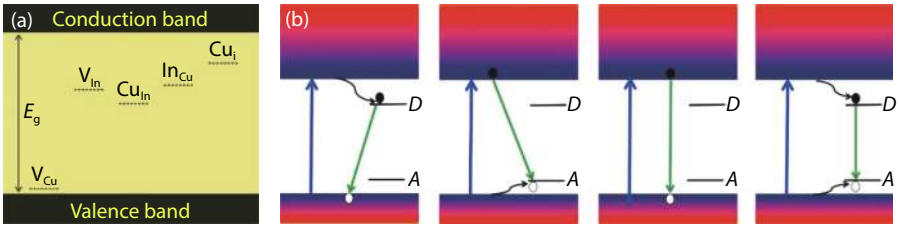

Fig. 5. (Color online) Schematic defect states[66] and charge carrier recombination pathways[67] of DAPs. Reprinted from Refs. [66, 67].

core/shell structured $CuInS_2$/ZnS with strong PL at short wavelengths, it is difficult to tell whether the spectral blue shift is the quantum size effect or caused by the introduction of wide-bandgap ZnS in alloy formation. With the increase of the ratio of zinc to copper, the absorbance and PL have a clear blue shift[72]. In optical studies, the band gap or E_{LUMO}–E_{HOMO} are often reported, but without the absolute position information of these levels. However, this information is essential for designing an efficient energy conversion system, including photovoltaics and photocatalysis. X-ray photoelectron spectroscopy (XPS) an be used to determine the VB position (or molecular HOMO orbital), while ultraviolet photoelectron spectroscopy (UPS) c for the CB position (or molecular LUMO orbital). Electrochemical method is another convenient approach for measuring redox potentials, which provides supplementary information beyond spectroscopic measurements, especially the surface states that affect the electron transportation on the electrode. However, careful considerations are still required regarding the electrochemical measurement of I–III–VI QDs.

5. Photocatalytic applications

5.1. General considerations

Band gap of I–III–VI QDs can be adjusted within a very wide range due to their composition manipulation capability, which represent the most promising visible-light-active photocatalysts for hydrogen production due to their excellent optoelectrical properties. Bulk I–III–VI sulfides were actually the first reported visible light photocatalysts with adjustable band gap used for photocatalytic water splitting[25, 73]. The early work of I–III–VI sulfide photocatalysts mainly focused on the effect of composition adjustment on photocatalytic performance, such as $(AgIn)_xZn_{2(1-x)}S_2$, $(CuIn)_{(x)}Zn_{2(1-x)}S_2$ and other solid solution materials. In 5s5p and Cu 3d/Ag 4d orbitals in I–III–VI sulfides can participate in the formation of CB and VB, respectively, giving continuously adjustable band gap over a wide range[74]. However, due to the complex composition and structure, the preparation usually requires high temperature annealing to increase crystallinity and reduce defects, which also results in its size increase and low specific surface area. For further improvement, nanostructuring can reduce the diffusion distance of the photo-generated charge carriers to the catalyst surface, and effectively improve the efficiency of surface hydrogen evolution reaction[75, 76]. Recently, researchers have developed simple hydrothermal and solvothermal methods to prepare high-specific surface area I–III–VI solid solution nanostructures, such as porous microspheres and hieratical nanostructures, which can provide a rich surface active sites[77]. Above all, high-crystallinity and small-size nanoparticles have always been the ideal structures pursued in photocatalytic applications. In addition to traditional composition and structure control, cocatalysts loading, and heterostructure construction strategies, the I–III–VI QDs also provide opportunities for size and surface ligand control, which provides unique advantages[36, 78–80]. In-depth systematic research on the composition and particle size of different systems is expected to screen out I–III–VI-based solid solution QDs photocatalysts with excellent performance, which is expected to greatly boost the visible light catalytic efficiency[14].

5.2. Size and shape control

For multinary I–III–VI QDs, the small size of QDs and the narrow band gap of sulfides have important effects on the photocatalytic water splitting technology. As the size decreases, the band structure of QDs changes from continuous to dis-

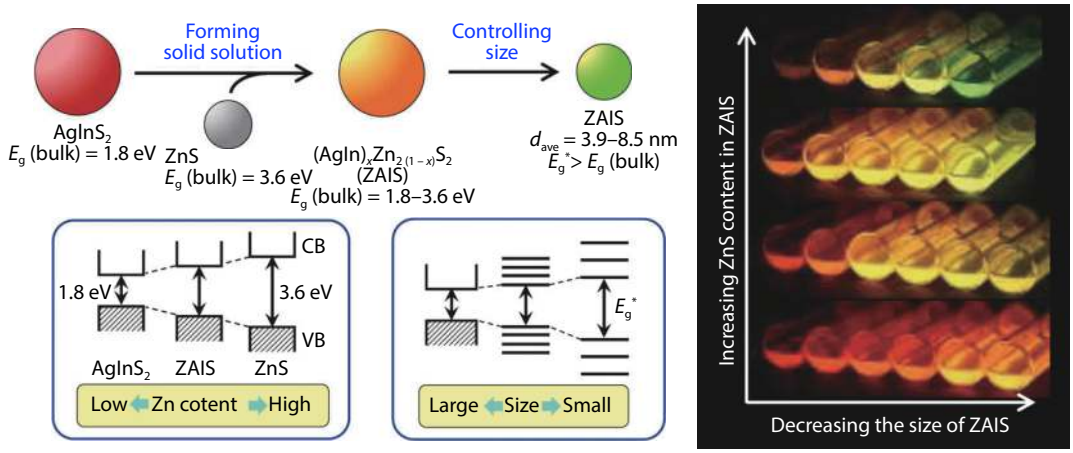

Fig. 6. (Color online) Size- and composition-dependent photocatalytic properties of ZAIS QDs. Reprinted from Ref. [85].

crete along with upshift of VB, resulting in the enhanced photoreduction capability, so reducing the size will usually facilitate photocatalytic H_2 production. The reduction in particle size results in larger surface area and more active sites on the surface[81–84]. However, it has also been reported that the number of surface traps and the nonradiative recombination decrease with increasing size to promote the photocatalytic water splitting. Kameyama *et al.* systematically explored how the size of $(AgIn)_xZn_{2(1-x)}S_2$ QDs affects the band structure and optical properties (Fig. 6), and found that the band gap narrows with increasing size, where the photocatalytic activity is optimal when the average size is 4.2–5.5 nm[85]. Shape control is another important factor for the I–III–VI QDs photocatalysts. One-dimensional (1D) nanostructures, such as elongated nanorods, are a promising type of photocatalyst that facilitates the charge separation and improves activity[84, 86–88]. Han *et al.* successfully prepared a series of elongated morphological nanostructures, such as $CuGaS_2$ tadpoles, $CuInS_2$ bullets, CuInZnS rods and Cu_2ZnGeS_4 worms[89].

5.3. Composition manipulation

Composition manipulation plays a critical role in I–III–VI QDs photocatalysts, not only for bang gap engineering, but also for catalytic activity. The band structure of the multinary compounds can be adjusted by composition, thereby affecting the light absorption ability and reduction ability to improve the photocatalytic performance (Fig. 6). Through theoretical calculation and analysis of energy band structure, it was found that Cu 3d or Ag 4d orbits play a critical role in the VB, while In 5s5p orbital constructs the CB of I–III–VI QDs[30]. For I–III–VI-based solid solutions, the introduction of Zn 4s4p orbital improves the CB level and improves the reducing capability of the photogenerated electrons[31]. A large number of studies on I–III–VI-based alloys have adjusted the band gap and the CB/VB positions via the ratio of metal cations to optimize the photocatalytic activity[14]. For example, Chen *et al.* pointed out that the $AgIn_5S_8$ photocatalyst with visible light response can perform photocatalytic hydrogen production at wavelengths greater than 640 nm[90]. I–III–VI-based solid solution QDs, such as ZnS–$AgInS_2$[91], $CuIn_{1-x}Ga_xS_2$[92] and $CuGa_2In_3S_8$[93], have shown excellent photocatalytic hydrogen production performance in recent studies. Among them, Yu *et al.* tested the influence of Ga content on catalytic activity of $CuIn_{1-x}Ga_xS_2$ QDs (optimized composition of $CuIn_{0.3}Ga_{0.7}S_2$)[94]. The hydrogen production rate of $CuGa_2In_3S_8$ QDs loading with Ru even exceeded the corresponding bulk material prepared by high temperature annealing method[95]. The introduction of Group I elements (Cu or Ag) is an effective means to reduce the band gap in the composition control of I–III–VI photocatalysts, but it also brings severe charge carrier recombination and thus reduced photocatalytic efficiency, resulting in the dilemma of unable to cooperate band gap narrowing and charge recombination. For this, Mao *et al.* reported that a proper amount of Ag doping (i.e. Ag : In < 1.5 : 10) can lead to continuous increase of photocatalytic hydrogen production, which achieved synergetic band gap narrowing and lifetime increase[74]. PL mechanism study shows that the ratio of intrinsic donor–acceptor state increases with moderate silver doping, beneficial to the lifetime elongation. This discovery provides a new perspective for narrow-band-gap photocatalysts[74].

5.4. Surface manipulation

The surface ligands not only determine the aqueous/organic dispersibility of the QDs, but may also serve as the surface catalytic center[96, 97]. Generally, the surface of QDs synthesized under the conditions of high temperature and high boiling point or organic solvent are often covered with a layer of organic ligands with long hydrocarbon tails (such as oleylamine, oleic acid and trioctylphosphine oxide)[98] to obtain high crystallinity and high dispersibility. They are easily dispersed in non-polar solvents or polymer matrix, but are difficult to disperse in aqueous phase. The pristine long-chain ligands are usually exchanged with short-chain bipolar ligands (such as 3-mercaptopropionic acid (MPA) or simple inorganic ions), which provide increased aqueous colloidal stability and convenient charge transport channels during photocatalysis beneficial for the photocatalytic activity. Lots of I–III–VI QDs photocatalysts were also directly prepared by aqueous methods with short-chain ligands. These short chain ligand-coated colloidal QDs exhibit better charge separation, high conductivity, and enhanced photocatalytic activity[99]. Moreover, Mao *et al.* found that Ag–In–Zn–S QDs modified with mixed ligands -shows an unexpected synergetic effect on the photocatalytic properties, where the introduction of MPA led to an increase in PL lifetime and a decrease in non-radiative recombination that can be attributed to the stronger caping effect of

MPA compared to that of L-cysteine[100]. Rao *et al.* found that simple S^{2-} ion coated $(ZnS)_{0.4}(AgInS_2)_{0.6}$ QDs have more active sites than the original QDs, thus making the photocatalytic activity increase[101].

5.5. Heterojunctions

In heterojunctions formed by combining semiconductor materials with different band gaps and energy levels, especially type-II heterojunctions, photogenerated electrons can transfer from high CB materials to relatively low CB materials, while photogenerated holes can migrate reversibly. This band arrangement thereby achieves efficient separation of electrons and holes. $CuIn_5S_8/Ag_2S$, $CuInSe_2/TiO_2$[102], $AgIn_5S_8/TiO_2$[103], $AgInS_2/ZnS$[104] and other heterojunctions have shown the capability to efficiently transfer the photo-generated electrons and holes, extend the carrier lifetime, and promote the photocatalytic performance of the composite. In-situ growth method is also reported for constructing 0D/2D heterojunctions, such as Zn–$AgIn_5S_8$QDs/g-C_3N_4 nanosheets[105].

5.6. Cocatalysts

Various cocatalysts, especially noble metals, are widely used as high-efficiency promoters in water splitting systems to enhance charge separation and catalytic activity. The Fermi level of the noble metals are often lower than that of the semiconductors and the electrons generated by the semiconductor can smoothly migrate to the active site of the precious metal to reduce the surface adsorbed H^+ to H_2[106]. The cocatalysts promote the separation of photo-generated carriers of semiconductor materials to a certain extent, which reduces the internal and surface electron/hole recombination. The reverse combination reaction is also suppressed to enhance the surface chemical reaction, and thus the photocatalytic performance is significantly improved. Various high-efficiency metal cocatalysts have loaded onto I–III–VI QDs, including Pt[107], Ru[108], Pd[109], and Rh[110]. In addition, adjusting the Cu content makes it easier to cover the entire solar spectrum, but it is often observed that even a relatively low Cu content will cause the photocatalyst to deactivate. Mao *et al.* recently found that loading Pt cocatalyst could cause a shift in the photocatalytic activity trend in a series of Cu–In–Zn–S QDs, where the optimized sample was changed from Cu/In/Zn of 0.1/10/5 without Pt to 1/10/5 with Pt, e.g. the tolerance to Cu doping was increased by 10 times[15]. This phenomenon is ascribed to the competitive effect of band gap narrowing by Cu doping, charge recombination by Cu defect sites and charge separation induced by Pt cocatalysts. In addition to noble metals, transition metal sulfides are a class of cocatalysts with outstanding performance in photocatalytic hydrogen production. Mao *et al.* pointed out that the introduction of MoS_2 nanosheets increased the photogenerated electron transfer of Zn–AgInS QDs and optimized the photocatalytic activity[111]. Ning *et al.* combined 0D AgInZnS QDs and 2D MoS_2 nanosheets to construct a heterojunction, and systesystematically explored the effects of the amount of Ag doping, sacrificial reagents, and MoS_2 co-catalyst loading on the photocatalytic activity. It was found that the introduction of the inexpensive MoS_2 nanosheets made the AQE up to 41% (at 400 nm) with a high hydrogen production rate of 40.1 mmol g^{-1} h^{-1}[112].

5.7. Stability and hole scarification

Photocorrosion caused by the oxidative holes is a problem faced by most narrow-band-gap sulfide photocatalysts[113]. Stability is still one of the biggest challenges for these narrow-bandgap sulfide QDs, similar to CdS and CdSe. It's worth to note that sulfides play a critical role for visible-light-driven photocatalysis, so the stability and photocorrosion issues have attracted lots of attention in traditional QDs photocatalysts. For example, in addition to the above-mentioned modification methods, other experimental conditions for photocatalytic water splitting (such as pH, temperature, sacrificial agents, etc.) also affect the hydrogen production activity of the photocatalysts. Lots of efforts have been contributed to the separation of the photogenerated charge carriers, such as heterojunction construction and use of hole sacrificial agents, such as S^{2-}/SO_3^{2-} and ascorbic acid. It has also been realized that hole trapping in the defect states is probably the main cause of photocorrosion, and corresponding strategies have started to be explored, such as surface defect engineering and hole accepting ligand modification, which are also learned from traditional QDs. For metal sulfide photocatalysts, S^{2-} and SO_3^{2-} mixtures are usually used as sacrificial agents to capture the photo-generated holes and thus minimize recombination between electrons and holes[114]. In the photocatalysis process, the holes oxidize S^{2-} to S as a competitive reaction to the photocorrosion of the catalyst themselves. The resulted dark-color S and S_2^{2-} will react with the SO_3^{2-} added to the system to form light-color $S_2O_3^{2-}$ and get eliminated to avoid light shielding effect. In addition to the Na_2S/Na_2SO_3 system, triethanolamine, L-cysteine, and ascorbic acid have also been widely explored as sacrificial agents for QDs-based hydrogen production[115].

6. Bridging between QDs and emerging carbon dots

As mentioned above, the QDs family has shown amazing developing vitality, and the connotation is also constantly expanding, bringing a series of new phenomena, new principles and new challenges to the QDs field. Now, as it expands from traditional II–VI semiconductors to carbon and other emerging materials, there is a huge gap in the composition and structure, leading to completely different synthetic chemistry, PL mechanisms and applications[23]. Thus, it is difficult for carbon dots to learn directly from traditional II–VI QDs. As a close relative of II–VI QDs, I–III–VI QDs still belong to traditional semiconductors, for which the principles of synthesis and structure are similar, but with more complicated composition and structural variations that brings new optoelectronic properties. From this point of view, their corresponding manipulating strategies and development history that are closely related with II–VI QDs but with new challenges, provide a opportunity to bridge the huge gap between traditional QDs and emerging new carbon dots. For photocatalysis, traditional QDs play an important role in the clarification of photocatalysis mechanisms and high-efficiency photocatalyst design, while carbon dots show unique charm in all the three aspects of photocatalysis, e.g. enhancing light absorption, charge transfer and co-catalysis. Carbon dots reflect the dual merits of small-size QDs and carbon materials, show high catalytic activity for many reactions, and can be used as

Table 1. Bridging between traditional II–VI QDs and emerging carbon dots by I–III–VI QDs.

	II–VI QDs	I–III–VI QDs	Carbon dots
Structure	Quasi-spherical[121] or faceted nanocrystalline core[122]	Quasi-spherical[123] or faceted nanocrystalline core[124]	Crystalline (graphitic)[125] or amorphous carbon core (often with irregular shape)[126]
	Capping ligands[127]	Capping ligands[8]	Surface functional groups[128]
	Stoichiometric composition	Nonstoichiometric composition[14]	Nonstoichiometric carbon core and surface[129]
	Mainly surface defects[130]	Abundant inner (intrinsic)/surface defects[131]	Multi energy levels and abundant inner/surface defects[132, 133]
Synthesis	Organometallic hot-injection method[134]	Organometallic hot-injection method[135, 136]	Both up-side-down[137] and bottom-up methods[138]
	Ionic reactions[139]	Ionic reactions[56]	Radical reactions[140]
	Precise size and shape control[141]	Challenging: balance of cation reactivity[142]	Challenging: difficult to control; prefer organic synthetic methods
	Relatively mature doping[143] and heterojunction[144] construction;	Competition of core/shell[145] vs. interfacial alloying[146];	Doping[147] and heterojunction[148] construction: lots of study but very difficult for precise control[149]
	Profound understanding of growth kinetics and synthetic chemistry	Difficult to obtain clear heterojuntions	Growth kinetics and synthetic chemistry: complicated reaction intermediates and byproducts[150]
Optical properties	Narrow PL peak[151], high PL QYs, small stokes shift, short lifetime (for band edge emission)[152]	New: large stokes shift, wide PL peak, long lifetime[152, 153]	New: excitation-dependent emission, wide PL peak (multi states), long lifetime (fl & pl), up conversion[154, 155]
	Quantum size effect: clear[156]	Quantum size effect[1]: challenging (composition-dependent)	Quantum size effect: unclear (unkown core composition & surface groups)
	Extinction coefficient: clear	Only $CuInS_2$[157]	No report
	Mechanism: interband recombination & surface defect trap states[158]	Mechanism: DAP recombination[159]	Mechanism: sp^2 domain-induced interband PL, surface molecular emission, AIE, etc.
	Band gap engineering[160] and wavefunction engineering[161]	Band gap engineering[162] and wave function engineering[163]: size-, composition and structure dependent[14]	Band gap engineering and wavefunction engineering: very challenging[154, 155]
Photocatalysis	Combined Homogeneous/ heterogeneous photocatalysis[164, 165]	Heavy metal free[166]	Contribute on light absorption[119, 167]
	High absorbance[160]; high surface area[168]	Continuous band gap tuning via composition[14]	Charge separation and cocatalysts[169, 170]
	Type-II heterojunction for efficient charge separation[171, 172]	Long lifetime[173]	Photogenerated e^-/h^+, photogenerated protons and photo-controlled electron transfer[23]
	Charge carrier dynamics:100% AQE	Delicate manipulation and utilization of intrinsic and surface defects[174]	Multi electron donating/accepting[175]

multi-functional compositions of many high-performance photocatalysts and electrocatalysts[116–119]. The unique structural advantages make carbon dots not only provide photo-generation e^-/h^+, but also provide photo-generated protons and photo-controlled electron transfer, which is useful in many organic catalytic reactions beyond photocatalysis[120]. Of course, the carbon dot-based catalysts are still in its infancy in terms of fine structure manipulation, ultrafast spectral mechanism and in-situ catalytic mechanism characterizations, which still has a large gap compared with traditional QDs. I–III–VI QDs photocatalysts have made great progress by learning from II–VI QDs, especially the concise manipulation of size, shape and surface, but also on their own advantages including continuous band gap tuning via composition, utilization of long-lived charge carriers and delicate manipulation of the intrinsic (e.g. DAPs) and surface defect states. This actually provides an opportunity for carbon dots to learn and consult, especially the composition tuning, defect manipulation and the implication of ultrafast spectroscopy on the complicated photocatalytic mechanisms. More detailed comparison is listed below in Table 1.

7. Conclusions

In summary, I–III–VI QDs own lots of unique structural and optical properties and play a key role in photoelectric fields, including photocatalysis. It has similar advantages and characteristics of traditional QDs, such as the size-dependent quantum confinement effect and high specific surface area. On one hand, traditional QDs have developed lots of useful strategies to improve light harvesting and charge separation, such as the delicate control over size, shape, surface exposure and heterostructures. On the other hand, these ternary or multinary I–III–VI QDs provide several characteristic advantages that traditional binary QDs do not have, especially the wide range regulation of composition and band gap, as well as the rich long-lived trap states, which greatly expands the design of solid solution QDs and composite photocatalysts with complex compositions and structures. However, the complicated composition also brought a series of challenges on the structure and synthesis of these QDs, such as the precise control of the composition, the balancing of cation reactivity, the unwanted cation exchange and diffusion for heterojunction construction. This may rely on the in-situ monitoring of the growing process and the deep understanding of the synthetic chemistry. Subsequently, more efforts are needed on the clarification of size- vs. composition-dependent band gap, the PL origin from the abundant trap states, the engineering and utilization of the long-lived charge carriers, which re-

quires investigation and manipulation of the excited states by ultrafast spectroscopy. As mentioned above, all structure controled methods of traditional QDs photocatalysts have been applied to the I–III–VI QDs system, including particle size, composition, surface ligands, cocatalysts, hole sacrificial agents, etc., which provide systematic research on related strategies as very good model system. In addition, the performance shortcomings of the traditional chalcogenide photocatalysts usually can also be found in the I–III–VI QDs system, such as poor stability, slow hole extraction, low charge carrier utilization efficiency, etc. These problems rely on ultrafast spectroscopic research, which also provides a good inspiration for other photocatalytic systems. In principle, photocatalysis is a special form of electrocatalysis, where the electrons and holes are provided by light irradiation. The advantages of I–III–VI QDs in mechanism research can also be extended to the entire photo/electrocatalysis fields Furthermore, as a natural multi-composition and multi-interface catalyst, I–III–VI QDs can be useful in the distribution process of active species, the adsorption of active species, and electron transfer in other catalytic systems in a much broader way. The identification and change of the active sites and other issues may provide useful help as a suitable model system for understanding the catalyst from the perspective of physical and chemical interface engineering, for which more profound ultrafast and in situ spectroscopy studies are the key. In terms of the overall significance of photocatalysis and other catalytic studies, I–III–VI QDs are a class of materials that far surpasses traditional binary QDs. With the joint efforts of researchers in related fields, we hope that they will play an increasingly important role in catalysis research.

Acknowledgements

This work is supported by the National Natural Science Foundation of China (21908081, 21501072, 51972216, 51725204, 21771132 and 52041202), the National MCF Energy R&D Program (2018YFE0306105), Innovative Research Group Project of the National Natural Science Foundation of China (51821002), the Jiangsu Specially-Appointed Professors Program, and the Natural Science Foundation of Jiangsu Province (BK20190041, BK20190828 and BK20150489).

References

[1] Li S Q, Tang X S, Zang Z G, et al. I–III–VI chalcogenide semiconductor nanocrystals: Synthesis, properties, and applications. Chin J Catal, 2018, 39(4), 590

[2] Kuo Y H, Lee Y K, Ge Y, et al. Strong quantum-confined Stark effect in germanium quantum-well structures on silicon. Nature, 2005, 437(7063), 1334

[3] Tae E L, Lee K E, Jeong J S, et al. Synthesis of diamond-shape titanate molecular sheets with different sizes and realization of quantum confinement effect during dimensionality reduction from two to zero. J Am Chem Soc, 2008, 130(20), 6534

[4] Cao Y, Guo J, Shi R, et al. Evolution of thiolate-stabilized Ag nanoclusters from Ag-thiolate cluster intermediates. Nat Commun, 2018, 9(1), 2379

[5] Ma H T, Pan L J, Wang J, et al. Synthesis of $AgInS_2$ QDs in droplet microreactors: Online fluorescence regulating through temperature control. Chin Chem Lett, 2019, 30(1), 79

[6] Stroyuk O, Raevskaya A, Spranger F, et al. Origin and dynamics of highly efficient broadband photoluminescence of aqueous glutathione-capped size-selected Ag–In–S quantum dots. J Phys Chem C, 2018, 122(25), 13648

[7] Oluwafemi O S, May B M M, Parani S, et al. Facile, large scale synthesis of water soluble $AgInSe_2$/ZnSe quantum dots and its cell viability assessment on different cell lines. Mat Sci Eng C, 2020, 106, 110181

[8] Zhu X S, Demillo V G, Chen S Q, et al. Development of non-cadmium I–III–VI quantum dots and their surface modification for biomedical applications. Mater Sci Forum, 2018, 915, 163

[9] Kalinowska D, Drozd M, Grabowska-Jadach I, et al. The influence of selected omega-mercaptocarboxylate ligands on physicochemical properties and biological activity of Cd-free, zinccopperindium sulfide colloidal nanocrystals. Mater Sci Eng C, 2019, 97, 583

[10] Chen B, Pradhan N, Zhong H. From large-scale synthesis to lighting device applications of ternary I–III–VI semiconductor nanocrystals: Inspiring greener material emitters. J Phys Chem Lett, 2018, 9(2), 435

[11] Yoon S Y, Kim J H, Kim K H, et al. High-efficiency blue and white electroluminescent devices based on non-Cd I–III–VI quantum dots. Nano Energy, 2019, 63, 103869

[12] Rui W, Xin T, Channa A I, et al. Environment-friendly Mn-alloyed core/shell quantum dots for high-efficiency photoelectrochemical cells. J Mater Chem A, 2020, 8(21), 10736

[13] Jalalah M, Al-Assiri M S, Park J G. One-pot gram-scale, eco-friendly, and cost-effective synthesis of $CuGaS_2$/ZnS nanocrystals as efficient UV-harvesting down-converter for photovoltaics. Adv Energy Mater, 2018, 8(20), 1703418

[14] Yarema O, Yarema M, Wood V. Tuning the composition of multicomponent semiconductor nanocrystals: The case of I–III–VI materials. Chem Mater, 2018, 30(5), 1446

[15] Tan L L, Liu Y H, Mao B D, et al. Effective bandgap narrowing of Cu–In–Zn–S quantum dots for photocatalytic H_2 production via cocatalyst-alleviated charge recombination. Inorg Chem Front, 2018, 5(1), 258

[16] Feng J, Yang X S, Feng G W, et al. The experimental determination of composition-dependent molar extinction coefficient of nonstoichiometric Zn–Cu–In–S nanocrystals. Mater Res Express, 2018, 5(7), 075030

[17] Nong J P, Lan G L, Jin W F, et al. Eco-friendly and high-performance photoelectrochemical anode based on $AgInS_2$ quantum dots embedded in 3D graphene nanowalls. J Mater Chem C, 2019, 7(32), 9830

[18] Stanbery B J. Copper indium selenides and related materials for photovoltaic devices. Crit Rev Solid State, 2002, 27(2), 73

[19] Feurer T, Reinhard P, Avancini E, et al. Progress in thin film CIGS photovoltaics - Research and development, manufacturing, and applications. Prog Photovolt, 2017, 25(7), 645

[20] Kameyama T, Kishi M, Miyamae C, et al. Wavelength-tunable band-edge photoluminescence of nonstoichiometric Ag–In–S nanoparticles via Ga^{3+} Doping. ACS Appl Mater Inter, 2018, 10(49), 42844

[21] Huang D, Jiang J W, Guo J, et al. General rules of the sub-band gaps in group-IV (Si, Ge, and Sn)-doped I–III–VI_2-type chalcopyrite compounds for intermediate band solar cell: A first-principles study. Mater Sci Eng B, 2018, 236–237, 147

[22] Chen M M, Xue H G, Guo S P. Multinary metal chalcogenides with tetrahedral structures for second-order nonlinear optical, photocatalytic, and photovoltaic applications. Coordin Chem Rev, 2018, 368(1), 115

[23] Liu Y H, Huang H, Cao W J, et al. Advances in carbon dots: from the perspective of traditional quantum dots. Mater Chem Front, 2020, 4(6), 1586

[24] Girma W M, Fahmi M Z, Permadi A, et al. Synthetic strategies and biomedical applications of I–III–VI ternary quantum dots. J Mater Chem B, 2017, 5(31), 6193

[25] Omata T, Nose K, Otsuka-Yao-Matsuo S. Size dependent optical band gap of ternary I–III–VI_2 semiconductor nanocrystals. J Appl Phys, 2009, 105(7), 073106

[26] Aldakov D, Lefrancois A, Reiss P. Ternary and quaternary metal chalcogenide nanocrystals: synthesis, properties and applications. J Mater Chem C, 2013, 1(24), 3756

[27] Wei S H, Ferreira L G, Zunger A. First-principles calculation of the order-disorder transition in chalcopyrite semiconductors. Phys Rev B, 1992, 45(5), 2533

[28] Sandroni M, Wegner K D, Aldakov D, et al. Prospects of chalcopyrite-type nanocrystals for energy applications. Acs Energy Lett, 2017, 2(5), 1076

[29] Nakamura H, Kato W, Uehara M, et al. Tunable photoluminescence wavelength of chalcopyrite $CuInS_2$-based semiconductor nanocrystals synthesized in a colloidal system. Chem Mater, 2006, 18(14), 3330

[30] Whitham P J, Marchioro A, Knowles K E, et al. Single-particle photoluminescence spectra, blinking, and delayed luminescence of colloidal $CuInS_2$ nanocrystals. J Phys Chem C, 2016, 120(30), 17136

[31] Takarabe K, Kawai K, Minomura S, et al. Electronic structure of some I–III–VI_2 chalcopyrite semiconductors studied by synchrotron radiation. J Appl Phys, 1992, 71(1), 441

[32] Zhang L L, Pan Z X, Wang W, et al. Copper deficient Zn–Cu–In–Se quantum dot sensitized solar cells for high efficiency. J Mater Chem A, 2017, 5(40), 21442

[33] Bouich A, Hartiti B, Ullah S, et al. Experimental, theoretical, and numerical simulation of the performance of $CuIn_xGa_{(1-x)}S_2$-based solar cells. Optik, 2019, 183, 137

[34] Pradeepkumar M S, Pal A S, Singh A, et al. Phase separation in wurtzite $CuIn_xGa_{1-x}S_2$ nanoparticles. J Mater Sci, 2020, 55(26), 11841

[35] Ilaiyaraja P, Mocherla P S, Srinivasan T K, et al. Synthesis of Cu-deficient and Zn-graded Cu–In–Zn–S quantum dots and hybrid inorganic-organic nanophosphor composite for white light emission. ACS Appl Mater Interfaces, 2016, 8(19), 12456

[36] Bujak P, Wrobel Z, Penkala M, et al. Highly luminescent Ag–In–Zn–S quaternary nanocrystals: Growth mechanism and surface chemistry elucidation. Inorg Chem, 2019, 58(2), 1358

[37] Tsolekile N, Parani S, Matoetoe M C, et al. Evolution of ternary I–III–VI QDs: Synthesis, characterization and application. Nano-Struct Nano-Objects, 2017, 12, 46

[38] Zhang R L, Yang P, Wang Y Q. Facile synthesis of $CuInS_2$/ZnS quantum dots with highly near-infrared photoluminescence via phosphor-free process. J Nanopart Res, 2013, 15(9), 1910

[39] Guan Z Y, Tang A W, Lv P W, et al. New insights into the formation and color-tunable optical properties of multinary Cu–In–Zn-based chalcogenide semiconductor nanocrystals. Adv Optical Mater, 2018, 6, 1701389

[40] Jiao M X, Li Y, Jia Y X, et al. Aqueously synthesized color-tunable quaternary Cu–In–Zn–S quantum dots for Cu(II) detection via mild and rapid cation exchange. Sens Actuators B, 2019, 294(1), 32

[41] Yang L, Antanovich A, Prudnikau A, et al. Highly luminescent Zn–Cu–In–S/ZnS core/gradient shell quantum dots prepared from indium sulfide by cation exchange for cell labeling and polymer composites. Nanotechnology, 2019, 30(39), 395603

[42] Connor S T, Hsu C M, Weil B D, et al. Phase transformation of biphasic Cu_2S–$CuInS_2$ to monophasic $CuInS_2$ nanorods. J Am Chem Soc, 2009, 131(13), 4962

[43] Torimoto T, Adachi T, Okazaki K, et al. Facile synthesis of ZnS–$AgInS_2$ solid solution nanoparticles for a color-adjustable luminophore. J Am Chem Soc, 2007, 129(41), 12388

[44] Chen Y Y, Wang Q, Zha T Y, et al. Green and facile synthesis of high-quality water-soluble Ag–In–S/ZnS core/shell quantum dots with obvious bandgap and sub-bandgap excitations. J Alloy Compd, 2018, 753(15), 364

[45] Masab M, Muhammad H, Shah F, et al. Facile synthesis of CdZnS QDs: Effects of different capping agents on the photoluminescence properties. Mat Sci Semicond Proc, 2018, 81, 113

[46] Mrad M, Ben Chaabane T, Rinnert H, et al. Aqueous synthesis for highly emissive 3-mercaptopropionic acid-capped AIZS quantum dots. Inorg Chem, 2020, 59(9), 6220

[47] Mao B D, Wang B, Yu F R, et al. Hierarchical MoS_2 nanoflowers on carbon cloth as an efficient cathode electrode for hydrogen evolution under all pH values. Int J Hydrogen Energ, 2018, 43(24), 11038

[48] Moradi Alvand Z, Rajabi H R, Mirzaei A, et al. Rapid and green synthesis of cadmium telluride quantum dots with low toxicity based on a plant-mediated approach after microwave and ultrasonic assisted extraction: Synthesis, characterization, biological potentials and comparison study. Mater Sci Eng C, 2019, 98, 535

[49] Hu X B, Chen T, Xu Y Q, et al. Hydrothermal synthesis of bright and stable $AgInS_2$ quantum dots with tunable visible emission. J Lumin, 2018, 200, 189

[50] Chen T, Hu X B, Xu Y Q, et al. Hydrothermal synthesis of highly fluorescent Ag–In–S/ZnS core/shell quantum dots for white light-emitting diodes. J Alloy Compd, 2019, 804(5), 119

[51] Das A, Snee P T. Synthetic developments of nontoxic quantum dots. Chemphyschem, 2016, 17(5), 598

[52] Li H, Chen Z H, Zhao L, et al. Synthesis of TiO_2@$ZnIn_2S_4$ hollow nanospheres with enhanced photocatalytic hydrogen evolution. Rare Met, 2019, 38(5), 420

[53] Kang X J, Yang Y C, Huang L J, et al. Large-scale synthesis of water-soluble $CuInSe_2$/ZnS and $AgInSe_2$/ZnS core/shell quantum dots. Green Chem, 2015, 17(8), 4482

[54] Cao W J, Qin Y L, Huang H, et al. Extraction of high-quality quantum dot photocatalysts via combination of size selection and electrochemiluminescence. Acs Sustain Chem Eng, 2019, 7(24), 20043

[55] Tessier M D, Baquero E A, Dupont D, et al. Interfacial oxidation and photoluminescence of InP-based core/shell quantum dots. Chem Mater, 2018, 30(19), 6877

[56] Li Y M, Liu J, Wan X D, et al. Surface passivation enabled-structural engineering of I–III–VI_2 nanocrystal photocatalysts. J Mater Chem A, 2020, 8(19), 9951

[57] Saidzhonov B M, Kozlovsky V F, Zaytsev V B, et al. Ultrathin CdSe/CdS and CdSe/ZnS core-shell nanoplatelets: The impact of the shell material on the structure and optical properties. J Lumin, 2019, 209, 170

[58] Yu K, Yang Y, Wang J, et al. Ultrafast carrier dynamics and third-order nonlinear optical properties of $AgInS_2$/ZnS nanocrystals. Nanotechnology, 2018, 29(25), 255703

[59] Michalska M, Aboulaich A, Medjahdi G, et al. Amine ligands control of the optical properties and the shape of thermally grown core/shell $CuInS_2$/ZnS quantum dots. J Alloy Compd, 2015, 645(5), 184

[60] Mao B D, Chuang C H, Lu F, et al. Study of the partial Ag-to-Zn cation exchange in $AgInS_2$/ZnS nanocrystals. J Phys Chem C, 2012, 117(1), 648

[61] Kim J H, Kim K H, Yoon S Y, et al. Tunable emission of bluish Zn–Cu–Ga–S quantum dots by Mn doping and their electroluminescence. ACS Appl Mater Inter, 2019, 11(8), 8250

[62] Paderick S, Kessler M, Hurlburt T J, et al. Synthesis and characterization of $AgGaS_2$ nanoparticles: A study of growth and fluorescence. Chem Commun, 2017, 54(1), 62

[63] Zhang K W, Liu Y H, Wang B, et al. Three-dimensional interconnected MoS_2 nanosheets on industrial 316 L stainless steel mesh as an efficient hydrogen evolution electrode. Int J Hydrogen Energ, 2019, 44(3), 1555

[64] Omata T, Nose K, Kurimoto K, et al. Electronic transition responsible for size-dependent photoluminescence of colloidal $CuInS_2$

quantum dots. J Mater Chem C, 2014, 2(33), 6867
[65] Mao B D, Chuang C H, Wang J W, et al. Synthesis and photophysical properties of ternary I–III–VI $AgInS_2$ nanocrystals: Intrinsic versus surface states. J Phys Chem C, 2011, 115(18), 8945
[66] Zhang S B, Wei S H, Zunger A. Defect physics of the $CuInSe_2$ chalcopyrite semiconductor. Phys Rev B, 1988, 57, 9642
[67] Debnath T, Ghosh H N. Ternary metal chalcogenides: Into the exciton and biexciton dynamics. J Phys Chem Lett, 2019, 10(20), 6227
[68] Leach A D, Macdonald J E. Optoelectronic properties of $CuInS_2$ nanocrystals and their origin. J Phys Chem Lett, 2016, 7(3), 572
[69] Liu W Y, Zhang Y, Zhao J, et al. Photoluminescence of indium-rich copper indium sulfide quantum dots. J Lumin, 2015, 162, 191
[70] Fuhr A, Yun H J, Crooker S A, et al. Spectroscopic and magneto-optical signatures of Cu^{1+} and Cu^{2+} defects in copper indium sulfide quantum dots. ACS Nano, 2020, 14(2), 2212
[71] Knowles K E, Hartstein K H, Kilburn T B, et al. Luminescent colloidal semiconductor nanocrystals containing copper: Synthesis, photophysics, and applications. Chem Rev, 2016, 116(18), 10820
[72] Zhong H Z, Lo S S, Mirkovic T, et al. Noninjection gram-scale synthesis of monodisperse pyramidal $CuInS_2$ nanocrystals and their size-dependent properties. ACS Nano, 2010, 4(9), 5253
[73] Rashkeev S N, Lambrecht W R L. Second-harmonic generation of I–III–VI_2 chalcopyrite semiconductors: Effects of chemical substitutions. Phys Rev B, 2001, 63(16), 165212
[74] Gong G, Liu Y H, Mao B D, et al. Ag doping of Zn–In–S quantum dots for photocatalytic hydrogen evolution: Simultaneous bandgap narrowing and carrier lifetime elongation. Appl Catal B, 2017, 216, 11
[75] Li Y, Zhang J Z. Hydrogen generation from photoelectrochemical water splitting based on nanomaterials. Laser Photonics Rev, 2009, 4(4), 517
[76] Jing L, Zhou W, Tian G, et al. Surface tuning for oxide-based nanomaterials as efficient photocatalysts. Chem Soc Rev, 2013, 42(24), 9509
[77] Ye Y, Zang Z G, Zhou T W, et al. Theoretical and experimental investigation of highly photocatalytic performance of CuInZnS nanoporous structure for removing the NO gas. J Catal, 2018, 357, 100
[78] Wang X L, Swihart M T. Controlling the size, shape, phase, band gap, and localized surface plasmon resonance of $Cu_{2-x}S$ and Cu_x-In_yS nanocrystals. Chem Mater, 2015, 27(5), 1786
[79] Yarema O, Yarema M, Moser A, et al. Composition- and size-controlled I–V–VI Semiconductor nanocrystals. Chem Mater, 2020, 32(5), 2078
[80] Mao B D, Chuang C H, Mccleese C, et al. Near-infrared emitting $AgInS_2$/ZnS nanocrystals. J Phys Chem C, 2014, 118(25), 13883
[81] Yarema O, Yarema M, Bozyigit D, et al. Independent composition and size control for highly luminescent indium-rich silver indium selenide nanocrystals. ACS Nano, 2015, 9(11), 11134
[82] Yarema O, Yarema M, Lin W M, et al. Cu–In–Te and Ag–In–Te colloidal nanocrystals with tunable composition and size. Chem Commun, 2016, 52(72), 10878
[83] Liu C, Li X, Li J, et al. Carbon dots modifying sphere-flower $CdIn_2S_4$ on N-rGO sheet muti-dimensional photocatalyst for efficient visible degradation of 2,4-dichlorophenol. J Taiwan Inst Chem E, 2019, 99, 142
[84] Zhu D X, Ye H H, Liu Z M. Seed-mediated growth of heterostructured $Cu_{1.94}S$–MS (M = Zn, Cd, Mn) and alloyed $CuNS_2$ (N = In, Ga) nanocrystals for use in structure- and composition-dependent photocatalytic hydrogen evolution. Nanoscale, 2020, 12, 6111
[85] Sharma D K, Hirata S, Bujak L, et al. Influence of Zn on the photoluminescence of colloidal $(AgIn)_xZn_{2(1-x)}S_2$ nanocrystals. Phys Chem Chem Phys, 2017, 19(5), 3963
[86] Ng M T, Boothroyd C B, Vittal J J. One-pot synthesis of new-phase $AgInSe_2$ nanorods. J Am Chem Soc, 2006, 128(22), 7118
[87] Liu Z, Liu J, Huang Y, et al. From one-dimensional to two-dimensional wurtzite $CuGaS_2$ nanocrystals: non-injection synthesis and photocatalytic evolution. Nanoscale, 2018, 11(1), 158
[88] Liu Z M, Tang A W, Liu J, et al. Non-injection synthesis of L-shaped wurtzite Cu–Ga–Zn–S alloyed nanorods and their advantageous application in photocatalytic hydrogen evolution. J Mater Chem A, 2018, 6, 18649
[89] Regulacio M D, Han M Y. Multinary I–III–VI_2 and I_2–II–IV–VI_4 semiconductor nanostructures for photocatalytic applications. Acc Chem Res, 2016, 49(3), 511
[90] Chen D, Ye J H. Photocatalytic H_2 evolution under visible light irradiation on $AgIn_5S_8$ photocatalyst. J Phys Chem Solids, 2007, 68, 2317
[91] Minoshima W, Ito R, Takiyama T, et al. Photoluminescence characterization of ZnS–$AgInS_2$ (ZAIS) nanoparticles adsorbed on plasmonic chip studied with fluorescence microscopy. J Photoch Photobio A, 2018, 367(1), 347
[92] Vasekar P S, Dhere N G. Effect of sodium addition on Cu-deficient $CuIn_{1-x}Ga_xS_2$ thin film solar cells. Sol Energ Mat Sol C, 2009, 93(1), 69
[93] Kandiel T A, Anjum D H, Takanabe K. Nano-sized quaternary $CuGa_2In_3S_8$ as an efficient photocatalyst for solar hydrogen production. ChemSusChem, 2014, 7(11), 3112
[94] Yu X L, An X Q, Shavel A, et al. The effect of the Ga content on the photocatalytic hydrogen evolution of $CuIn_{1-x}Ga_xS_2$ nanocrystals. J Mater Chem A, 2014, 2(31), 12317
[95] Kandiel T A, Hutton G A M, Reisner E. Visible light driven hydrogen evolution with a noble metal free $CuGa_2In_3S_8$ nanoparticle system in water. Catal Sci Technol, 2016, 6(17), 6536
[96] Hirase A, Hamanaka Y, Kuzuya T. Ligand-induced luminescence transformation in $AgInS_2$ nanoparticles: From defect emission to band-edge emission. J Phys Chem Lett, 2020, 11(10), 3969
[97] Peng Y, Shang L, Cao Y, et al. Effects of surfactants on visible-light-driven photocatalytic hydrogen evolution activities of AgIn-Zn_7S_9 nanorods. Appl Surf Sci, 2015, 358, 485
[98] Jung S, Cha J H, Jung D Y. Synthesis of oleic acid-capped $CuInS_2$ nanocrystals from bimetallic hydroxide precursor. Thin Solid Films, 2016, 603(31), 243
[99] Yu S, Fan X B, Wang X, et al. Efficient photocatalytic hydrogen evolution with ligand engineered all-inorganic InP and InP/ZnS colloidal quantum dots. Nat Commun, 2018, 9(1), 4009
[100] Yang Y L, Liu Y H, Mao B D, et al. Facile surface engineering of Ag–In–Zn–S quantum dot photocatalysts by mixed-ligand passivation with improved charge carrier lifetime. Catal Lett, 2019, 149(7), 1800
[101] Jagadeeswararao M, Dey S, Nag A, et al. Visible light-induced hydrogen generation using colloidal $(ZnS)_{0.4}(AgInS_2)_{0.6}$ nanocrystals capped by S^{2-} ions. J Mater Chem A, 2015, 3(16), 8276
[102] Kshirsagar A S, Gautam A, Khanna P K. Efficient photo-catalytic oxidative degradation of organic dyes using $CuInSe_2$/TiO_2 hybrid hetero-nanostructures. J Photoch Photobio A, 2017, 349(1), 73
[103] Li K, Chai B, Peng T Y, et al. Preparation of $AgIn_5S_8$/TiO_2 heterojunction nanocomposite and its enhanced photocatalytic H_2 production property under visible light. Acs Catal, 2013, 3(2), 170
[104] Kobosko S M, Jara D H, Kamat P V. $AgInS_2$–ZnS quantum dots: Excited state interactions with TiO_2 and photovoltaic performance. ACS Appl Mater Inter, 2017, 9(39), 33379
[105] Yang Y L, Mao B D, Gong G, et al. In-situ growth of Zn–$AgIn_5S_8$ quantum dots on g-C_3N_4 towards 0D/2D heterostructured photocatalysts with enhanced hydrogen production. Int J Hydrogen Energy, 2019, 44(30), 15882
[106] Subramanian V, Wolf E E, Kamat P V. Catalysis with TiO_2/gold nanocomposites. Effect of metal particle size on the Fermi level equilibration. J Am Chem Soc, 2004, 126(15), 4943

[107] Lan M, Guo R M, Dou Y B, et al. Fabrication of porous Pt-doping heterojunctions by using bimetallic MOF template for photocatalytic hydrogen generation. Nano Energy, 2017, 33, 238
[108] Iervolino G, Vaiano V, Sannino D, et al. Enhanced photocatalytic hydrogen production from glucose aqueous matrices on Ru-doped $LaFeO_3$. Appl Catal B, 2017, 207, 182
[109] Xue F, Chen C, Fu W L, et al. Interfacial and dimensional effects of Pd Co-catalyst for efficient photocatalytic hydrogen generation. J Phys Chem C, 2018, 122(44), 25165
[110] Huang J Q, Li G J, Zhou Z F, et al. Efficient photocatalytic hydrogen production over Rh and Nb codoped TiO_2 nanorods. Chem Eng J, 2018, 337(1), 282
[111] Gong G, Liu Y H, Mao B D, et al. Mechanism study on the photocatalytic efficiency enhancement of MoS_2 modified Zn–$AgIn_5S_8$ quantum dots. Rsc Adv, 2016, 6(101), 99023
[112] Huang T, Chen W, Liu T Y, et al. Hybrid of AgInZnS and MoS_2 as efficient visible-light driven photocatalyst for hydrogen production. Int J Hydrogen Energ, 2017, 42(17), 12254
[113] Zhen W L, Ning X F, Yang B J, et al. The enhancement of CdS photocatalytic activity for water splitting via anti-photocorrosion by coating Ni_2P shell and removing nascent formed oxygen with artificial gill. Appl Catal B, 2018, 221, 243
[114] Daskalaki V M, Antoniadou M, Puma G L, et al. Solar light-responsive Pt/CdS/TiO_2 photocatalysts for hydrogen production and simultaneous degradation of inorganic or organic sacrificial agents in wastewater. Energ Environ Sci, 2010, 44(19), 7200
[115] Wang M J, Shen S L, Li L, et al. Effects of sacrificial reagents on photocatalytic hydrogen evolution over different photocatalysts. J Mater Sci, 2017, 52(9), 5155
[116] Zhang J, Chen J W, Luo Y, et al. Sandwich-like electrode with tungsten nitride nanosheets decorated with carbon dots as efficient electrocatalyst for oxygen reduction. Appl Surf Sci, 2019, 466(1), 911
[117] Ding P, Di J, Chen X, et al. S, N codoped graphene quantum dots embedded in $(BiO)_2CO_3$: Incorporating enzymatic-like catalysis in photocatalysis. Acs Sustain Chem Eng, 2018, 6(8), 10229
[118] Ji M, Liu Y, Di J, et al. N-CQDs accelerating surface charge transfer of $Bi_4O_5I_2$ hollow nanotubes with broad spectrum photocatalytic activity. Appl Catal B, 2018, 237, 1033
[119] Miao X, Yue X, Ji Z, et al. Nitrogen-doped carbon dots decorated on g-C_3N_4/Ag_3PO_4 photocatalyst with improved visible light photocatalytic activity and mechanism insight. Appl Catal B, 2018, 227, 459
[120] Zhou Y Q, Zahran E M, Quiroga B A, et al. Size-dependent photocatalytic activity of carbon dots with surface-state determined photoluminescence. Appl Catal B, 2019, 248, 157
[121] Vaneski A, Schneider J, Susha A S, et al. Colloidal hybrid heterostructures based on II–VI semiconductor nanocrystals for photocatalytic hydrogen generation. J Photoch Photobio C, 2014, 19, 52
[122] Houtepen A J, Hens Z, Owen J S, et al. On the origin of surface traps in colloidal II–VI semiconductor nanocrystals. Chem Mater, 2017, 29(2), 752
[123] Ou K L, Fan J C, Chen J K, et al. Hot-injection synthesis of monodispersed $Cu_2ZnSn(S_xSe_{1-x})_4$ nanocrystals: Tunable composition and optical properties. J Mater Chem, 2012, 22(29), 14667
[124] Ren H, Wang M, Li Z, et al. Synthesis and characterization of $CuZnSe_2$ nanocrystals in wurtzite, zinc blende, and core–shell polytypes. Chem Mater, 2019, 31(24), 10085
[125] Liu W, Li C, Sun X, et al. Highly crystalline carbon dots from fresh tomato: UV emission and quantum confinement. Nanotechnology, 2017, 28(48), 485705
[126] Wu P, Wu X Y, Li W, et al. Ultra-small amorphous carbon dots: preparation, photoluminescence properties, and their application as TiO_2 photosensitizers. J Mater Sci, 2018, 54(7), 5280
[127] Ingole P P. A consolidated account of electrochemical determination of band structure parameters in II–VI semiconductor quantum dots: a tutorial review. Phys Chem Chem Phys, 2019, 21(9), 4695
[128] Miao X, Qu D, Yang D, et al. Synthesis of carbon dots with multiple color emission by controlled graphitization and surface functionalization. Adv Mater, 2018, 30(1), 1704740
[129] Hu S, Trinchi A, Atkin P, et al. Tunable photoluminescence across the entire visible spectrum from carbon dots excited by white light. Angew Chem Int Ed Engl, 2015, 54(10), 2970
[130] Qi H, Wang S J, Jiang X H, et al. Research progress and challenges of blue light-emitting diodes based on II–VI semiconductor quantum dots. J Mater Chem C, 2020
[131] Du J, Singh R, Fedin I, et al. Spectroscopic insights into high defect tolerance of Zn:$CuInSe_2$ quantum-dot-sensitized solar cells. Nat Energy, 2020, 5(5), 409
[132] Xu X Y, Bao Z J, Tang W S, et al. Surface states engineering carbon dots as multi-band light active sensitizers for ZnO nanowire array photoanode to boost solar water splitting. Carbon, 2017, 121, 201
[133] Yan F, Sun Z, Zhang H, et al. The fluorescence mechanism of carbon dots, and methods for tuning their emission color: A review. Mikrochim Acta, 2019, 186(8), 583
[134] Lee Y S, Bu H B, Taniguchi T, et al. Hydrothermal synthesis of NAC-capped II–VI semiconductor ZnSe quantum dots in acidic condition. Chem Lett, 2016, 45(8), 878
[135] Ghali M, Rezk A, Eissa A M, et al. Hot-injection synthesis of ultrasmall $CuIn_3Se_5$ quantum dots and production of ink-coated films. J Phys Chem Solids, 2020, 146, 109610
[136] Shang L, Zhou C, Bian T, et al. Facile synthesis of hierarchical Zn-In_2S_4 submicrospheres composed of ultrathin mesoporous nanosheets as a highly efficient visible-light-driven photocatalyst for H_2 production. J Mater Chem A, 2013, 1(14), 4552
[137] Delfin F A, Bruhl S P, Forsich C, et al. Carbon based DLC films: Influence of the processing parameters on the structure and properties. Materia-Brazil, 2018, 23(2), 1517
[138] Rigodanza F, Dordevic L, Arcudi F, et al. Customizing the electrochemical properties of carbon nanodots by using quinones in bottom-up synthesis. Angew Chem Int Ed, 2018, 57(18), 5062
[139] Agarwal R, Krook N M, Ren M L, et al. Anion exchange in II–VI semiconducting nanostructures via atomic templating. Nano Lett, 2018, 18(3), 1620
[140] Ren X Y, Liang W X, Wang P, et al. A new approach in functionalization of carbon nanoparticles for optoelectronically relevant carbon dots and beyond. Carbon, 2019, 141, 553
[141] Kumar S, Nann T. Shape control of II–VI semiconductor nanomaterials. Small, 2006, 2(3), 316
[142] Xie R G, Rutherford M, Peng X G. Formation of high-quality I–III–VI semiconductor nanocrystals by tuning relative reactivity of cationic precursors. J Am Chem Soc, 2009, 131(15), 5691
[143] Du Fosse I, Ten Brinck S, Infante I, et al. Role of surface reduction in the formation of traps in n-doped II–VI semiconductor nanocrystals: How to charge without reducing the surface. Chem Mater, 2019, 31(12), 4575
[144] Zhan Y Y, Shao Z B, Jiang T H, et al. Cation exchange synthesis of two-dimensional vertical Cu_2S/CdS heterojunctions for photovoltaic device applications. J Mater Chem A, 2020, 8(2), 789
[145] Jain S, Bharti S, Bhullar G K, et al. I–III–VI core/shell QDs: Synthesis, characterizations and applications. J Lumin, 2020, 219, 116912
[146] Zhang A, Dong C, Li L, et al. Non-blinking (Zn)CuInS/ZnS quantum dots prepared by in situ interfacial alloying approach. Sci Rep, 2015, 5, 15227
[147] Li L B, Dong T. Photoluminescence tuning in carbon dots: surface passivation or/and functionalization, heteroatom doping. J Mater Chem C, 2018, 6(30), 7944
[148] Hu S, Yang W, Li N, et al. Carbon-dot-based heterojunction for en-

gineering band-edge position and photocatalytic performance. Small, 2018, 14(44), 1803447
[149] Yao B W, Huang H, Liu Y, et al. Carbon dots: A small conundrum. Trends Chem, 2019, 1(2), 235
[150] Ludmerczki R, Mura S, Carbonaro C M, et al. Carbon dots from citric acid and its intermediates formed by thermal decomposition. Chem-Eur J, 2019, 25(51), 11963
[151] Asano H, Tsukuda S, Kita M, et al. Colloidal Zn(Te,Se)/ZnS core/shell quantum dots exhibiting narrow-band and green photoluminescence. ACS Omega, 2018, 3(6), 6703
[152] Kameyama T, Sugiura K, Ishigami Y, et al. Rod-shaped Zn–Ag–In–Te nanocrystals with wavelength-tunable band-edge photoluminescence in the near-IR region. J Mater Chem C, 2018, 6(8), 2034
[153] Huang H Y, Cai K B, Chen P W, et al. Engineering ligand–metal charge transfer states in cross-linked gold nanoclusters for greener luminescent solar concentrators with solid-state quantum yields exceeding 50% and low reabsorption losses. J Phys Chem C, 2018, 122(34), 20019
[154] Wang C, Chen Y, Hu T, et al. Color tunable room temperature phosphorescent carbon dot based nanocomposites obtainable from multiple carbon sources via a molten salt method. Nanoscale, 2019, 11(24), 11967
[155] Ding H, Wei J S, Zhang P, et al. Solvent-controlled synthesis of highly luminescent carbon dots with a wide color gamut and narrowed emission peak widths. Small, 2018, 14(22), 1800612
[156] Mansur A A P, Mansur H S, Mansur R L, et al. Bioengineered II–VI semiconductor quantum dot-carboxymethylcellulose nanoconjugates as multifunctional fluorescent nanoprobes for bioimaging live cells. Spectrochim Acta A, 2018, 189(15), 393
[157] Xia C, Wu W, Yu T, et al. Size-dependent band-gap and molar absorption coefficients of colloidal $CuInS_2$ quantum dots. ACS Nano, 2018, 12(8), 8350
[158] Li J Z, Chen J L, Shen Y M, et al. Extinction coefficient per CdE (E = Se or S) unit for zinc-blende CdE nanocrystals. Nano Research, 2018, 11(8), 3991
[159] Hu J H, Song J L Q, Tang Z S, et al. Phospholipid-stabilized $Cu_xAg_{1-x}InSe_2$ nanocrystals as luminophores: fabrication, optical properties, and biological application. J Mater Chem C, 2020, 8(17), 5821
[160] Lu J, Liu H, Zhang X, et al. One-dimensional nanostructures of II–VI ternary alloys: synthesis, optical properties, and applications. Nanoscale, 2018, 10(37), 17456
[161] Wieliczka B M, Kaledin A L, Buhro W E, et al. Wavefunction engineering in CdSe/PbS core/shell quantum dots. ACS Nano, 2018, 12(6), 5539
[162] Wu Y J, Zhang Y, Sui Y R, et al. Bandgap engineering of $Cu_2In_xZn_{1-x}Sn(S,Se)_4$ alloy films for photovoltaic applications. Ceram Int, 2018, 44(2), 1942
[163] Sun J, An L, Xue G, et al. Wavefunction engineering for efficient photoinduced-electron transfer in $CuInS_2$ quantum dot-sensitized solar cells. Nanotechnology, 2020, 31(21), 215408
[164] Chen Y Z, Li W H, Li L, et al. Progress in organic photocatalysts. Rare Met, 2017, 37(1), 1
[165] Liu X, Yan Y, Da Z, et al. Significantly enhanced photocatalytic performance of CdS coupled nanosheets and the mechanism study. Chem Eng J, 2014, 241, 243
[166] Meinardi F, Mcdaniel H, Carulli F, et al. Highly efficient large-area colourless luminescent solar concentrators using heavy-metal-free colloidal quantum dots. Nat Nanotechnol, 2015, 10(10), 878
[167] Li J, Liu K, Xue J, et al. CQDs preluded carbon-incorporated 3D burger-like hybrid ZnO enhanced visible-light-driven photocatalytic activity and mechanism implication. J Catal, 2019, 369, 450
[168] Mazzio K A, Prasad S K K, Okamoto K, et al. End-functionalized semiconducting polymers as reagents in the synthesis of hybrid II–VI nanoparticles. Langmuir, 2018, 34(33), 9692
[169] Meng X B, Sheng J L, Tang H L, et al. Metal-organic framework as nanoreactors to co-incorporate carbon nanodots and CdS quantum dots into the pores for improved H_2 evolution without noble-metal cocatalyst. Appl Catal B, 2019, 244, 340
[170] Di J, Xia J, Huang Y, et al. Constructing carbon quantum dots/Bi_2SiO_5 ultrathin nanosheets with enhanced photocatalytic activity and mechanism investigation. Chem Eng J, 2016, 302, 334
[171] Zhukovskyi M, Yashan H, Kuno M. Low-dimensional II–VI semiconductors for photocatalytic hydrogen generation. Res Chem Intermed, 2019, 45(8), 4249
[172] Qin Y, Li H, Lu J, et al. Nitrogen-doped hydrogenated TiO_2 modified with CdS nanorods with enhanced optical absorption, charge separation and photocatalytic hydrogen evolution. Chem Eng J, 2020, 384, 123275
[173] Jiao M, Li Y, Jia Y, et al. Strongly emitting and long-lived silver indium sulfide quantum dots for bioimaging: Insight into co-ligand effect on enhanced photoluminescence. J Colloid Interface Sci, 2020, 565, 35
[174] Fan F J, Wu L, Yu S H. Energetic I–III–VI_2 and I_2–II–IV–VI_4 nanocrystals: synthesis, photovoltaic and thermoelectric applications. Energ Environ Sci, 2014, 7(1), 190
[175] Ansi V A, Vijisha K R, Muraleedharan K, et al. Fluorescent carbon nanodots as efficient nitro aromatic sensor- analysis based on computational perspectives. Sens Actuators A, 2020, 302(1), 111817